

Article

# Porous Polymers Based on 9,10-Bis(methacryloyloxymethyl)anthracene—Towards Synthesis and Characterization

Małgorzata Maciejewska \* and Mateusz Józwicki 

Department of Polymer Chemistry, Institute of Chemical Sciences, Faculty of Chemistry, Maria Curie-Skłodowska University in Lublin, Gliniana 33, 20-614 Lublin, Poland

\* Correspondence: mmacieje@umcs.pl

**Abstract:** Porous materials can be found in numerous essential applications. They are of particular interest when, in addition to their porosity, they have other advantageous properties such as thermal stability or chemical diversity. The main aim of this study was to synthesize the porous copolymers of 9,10-bis(methacryloyloxymethyl)anthracene (BMA) with three different co-monomers divinylbenzene (DVB), ethylene glycol dimethacrylate (EGDMA) and trimethylpropane trimethacrylate (TRIM). They were synthesized via suspension polymerization using chlorobenzene and toluene served as porogenic solvents. For the characterization of the synthesized copolymers ATR-FTIR spectroscopy, a low-temperature nitrogen adsorption–desorption method, thermogravimetry, scanning electron microscopy, inverse gas chromatography and size distribution analysis were successfully employed. It was found that depending on the used co-monomer and the type of porogen regular polymeric microspheres with a specific surface area in the range of 134–472 m<sup>2</sup>/g can be effectively synthesized. The presence of miscellaneous functional groups promotes divergent types of interactions. Moreover, all of the copolymers show a good thermal stability up to 307 °C. What is important, thanks to application of anthracene derivatives as the functional monomer, the synthesized materials show fluorescence under UV radiation. The obtained microspheres can be used in various adsorption techniques as well as precursor for thermally resistant fluorescent sensors.

**Keywords:** polymeric microspheres; porous structure; thermal resistance



**Citation:** Maciejewska, M.; Józwicki, M. Porous Polymers Based on 9,10-Bis(methacryloyloxymethyl)anthracene—Towards Synthesis and Characterization. *Materials* **2023**, *16*, 2610. <https://doi.org/10.3390/ma16072610>

Academic Editor: Jie He

Received: 28 February 2023

Revised: 15 March 2023

Accepted: 22 March 2023

Published: 25 March 2023



**Copyright:** © 2023 by the authors. Licensee MDPI, Basel, Switzerland. This article is an open access article distributed under the terms and conditions of the Creative Commons Attribution (CC BY) license (<https://creativecommons.org/licenses/by/4.0/>).

## 1. Introduction

Porous materials play a crucial role in a modern society. A variety of contemporary achievements relies on porous components. These materials are successfully utilized as column packing in different chromatography techniques [1–9], as filtration/separation membranes [10,11], as support for sensors and catalysts [12–14], as transporters in drug delivery systems [15–17]. They are also widely applied for detection and removal of pollutants from water [18,19], for CO<sub>2</sub> capture [20,21], separation of rare earth elements [22] and many others advanced applications [23–29]. Porous materials can be obtained either by creating small particles or clusters where the surface-to-volume ratio of each particle is high, or by producing materials where the void surface area (pores) is high compared to the number of particles. These pores can be created through different methods, such as using a porogen during polymerization, or by post-processing the polymer. As a result, an amazing variety of porous products is constantly created and implemented. To improve tracking down and analysis of this impressive class of materials, various types of classifications are applied by scientists around the world. One of the commonly accepted division includes three main groups. Firstly, natural materials with high surface area. There are several natural materials that have a strongly developed internal surface such as, zeolites, clays, pumice, peat, metal oxides or activated charcoal. Zeolites are naturally occurring minerals that have a high surface area and a porous structure. They are composed of

aluminum, silicon, and oxygen, and are characterized by a three-dimensional network of tetrahedrally coordinated aluminum and silicon atoms. The pores in zeolites are typically in the range of 0.3 to 1 nanometer in diameter. They are widely used in catalysis, organic synthesis, solar energy storage and use, gas separation and other chemical and biomedical application [30,31]. In the case of clays, their structure significantly varies as a result of the function of the mineralogical reserve. What is important, on the basis of clay minerals, more advanced porous clay heterostructures (PCH) can be easily obtained. PCH materials were studied as catalysts of various reactions, as adsorbent for CO<sub>2</sub> capture, removal of heavy metal and dyes [32–36]. In turn, peat is a soil-like material that is composed of partially decomposed plant material. Peat has a high surface area, a relatively high water-holding capacity, and a spongy texture. For dyes and metals in wastewater, it can be used as an adsorbent [37]. However, the oldest and still extensively utilized natural adsorbents are porous carbons. They have been among the most explored materials due to their low cost, good stability, and high specific surface areas [38–40]. The second significant group are metal–organic frameworks (MOFs). These structures are made up of organic linkers that are held together by metal atoms. As a result, they look like a molecular cage. The metal ions or clusters provide the framework, while the organic ligands provide the porosity. This combination of metal ions or clusters and organic ligands creates a highly porous structure with a large surface area. They are used in desalination, carbon capture and storage, gas separation, biological imaging and sensing and play many other essential function [41–45].

Finally, permanently porous polymers. These highly cross-linked, three-dimensional networks possess superior inherent porosity, excellent stability, pre-designable and tunable structures. They are a broad class of advanced materials that have gained remarkable attention [46–50]. Porous polymers are mainly obtained during the radical copolymerization with cross-linking with the presence of diluents. At a certain degree of conversion, the homogeneous polymerization mixture is separated into solid and liquid phases: The solid phase is made up of a cross-linked polymer network, whereas of the solvent and unreacted comonomers consist liquid phase. The process of phase separation occurs. It is determined by the increase in cross-linking degree ( $\nu$ -syneresis) or the alternation interactions of polymer-solvent ( $\chi$ -syneresis). In the second case, it can be macro- or microsineresis. In the case of microsineresis, the liquid phase is dispersed in the continuous phase of polymer gel. During macrosineresis, the nuclei aggregated. They are microgels of higher a degree of cross-linking surrounded by a liquid phase. The resulting microgels react with each other by free vinyl bonds to form agglomerates (macrogels). The free volume between agglomerates creates macropores that is, according to the IUPAC recommendation [51], pores larger than 50 nm in diameters. Mesopores with pore size in the range of 2–50 nm can be found between macrogels and micropores (linear dimension below 2 nm) are present between microgels. Generally, porous polymers display micro-, meso- and macroporosity, which supports diversified application. The high microporosity of polymers allows them to be used in the adsorption and separation of small hydrocarbons or CO<sub>2</sub>. The mesoporosity make them excellent candidates for catalysts or catalytic supports due to their high specific surface area and high stability. Additionally, the mesoporosity also support the adsorption of big molecules, such as aromatic compounds. Due to the presence of macroporosity, the polymers have a high potential for the adsorption of large molecules such as dyestuff or complex biomolecules.

A significant variety of the polymer implementation creates a need for materials which possesses distinct or even conflicting properties. In our approach, we targeted into polymeric microspheres with considerably developed porous structure, diversified functional group and high thermal stability. As indicated in our previous study [52] synthesis of porous copolymers based on aromatic divinylbenzene (DVB) with different comonomers leads to materials with a good thermal resistance. For all synthesized materials, the  $T_{5\%}$  determined in helium atmosphere was above 300 °C: Following this strategy, we used a tetrafunctional methacrylate monomer based on anthracene, i.e., 9,10-bis(methacryloyloxymethyl)anthracene (BMA). BMA is a methacrylic derivative of

anthracene, an important representative of polycyclic aromatic hydrocarbons (PAH). Anthracene contains three fused benzene rings. The aromatic rings that form the monomer structure provide the  $\pi$ - $\pi$  interactions. Anthracene is colorless but exhibits fluorescence under ultraviolet radiation so it can be easily used as a UV tracer, e.g., in the conformal coatings applied in printed wiring boards [53]. Similar behavior can be observed for other polycyclic aromatic hydrocarbons. The simplest PAH is naphthalene. Its derivative, i.e., naphthalene-2,7-diol was used to synthesis the reactive monomer 2,7-di(methacryloyloxy)naphthalene. After excitation by UV radiation, it emits yellow radiation. It was successfully applied in the copolymerization with 2-hydroxyethyl methacrylate, N-vinyl-2-pyrrolidone, styrene, 1,4-divinylbenzene and methyl methacrylate [54]. Additionally, the synthesis of aromatic thiomethacrylate derivatives of naphthalene and their copolymers was reported [55]. It was of interest to test the possibility of BMA application in synthesis of fluorescent porous copolymers in the form of microspheres. The proper selection of the polymerization technique allows to obtain microspheres with a wide spectrum of diameters. The main factor that determines the choice of the suitable method is the potential application. In the case of some essential techniques (e.g., PALS studies, gas chromatography, catalysis), the required size of the microspheres is about 100  $\mu\text{m}$ . In order to achieve the desired diameter of the porous copolymers, the suspension technique is commonly employed. The suspension polymerization takes place under the influence of an initiator dissolved in the monomers dispersed in an aqueous solution stabilized by a proper agent. The type and amount of the stabilizers determines the size and quality of the microspheres. Based on our earlier studies [56,57], it was found out that polyvinyl alcohol of molecular weight 72,000 is a stabilizer that allows to obtain polymer microspheres having the desired diameter and perfectly spherical shape. However, the applied amount (6.5 g/195 mL H<sub>2</sub>O) generated some problems with the effective removal of the stabilizer. In this study, we decided to investigate the influence of stabilizer concentration on the quality of the synthesized microspheres. The main goal was to achieve regular, porous, highly crosslinked microspheres based on 9,10-bis(methacryloyloxymethyl)anthracene (BMA).

As co-monomers divinylbenzene (DVB), ethylene glycol dimethacrylate (EGDMA), and trimethylpropane trimethacrylate (TRIM) were applied. Chlorobenzene and toluene served as porogenic solvents. The obtained copolymers were thoroughly characterized by ATR-FTIR spectroscopy, thermogravimetry, scanning electron microscopy, a low-temperature nitrogen adsorption–desorption method, and size distribution analysis.

## 2. Materials and Methods

### 2.1. Chemicals

TRIM from Sigma-Aldrich (Schnelldorf, Germany), DVB and EGDMA from Merck (Darmstadt, Germany) were washed with 5% aqueous sodium hydroxide to remove inhibitors. Poly(vinyl alcohol) (PVA, MW 72,000) and 2,2'-azoisobutyronitrile (AIBN) achieved from Fluka (Buchs, Switzerland) were used as received. Reagent grade acetone, toluene, chlorobenzene, benzene, butan-1-ol, methanol, pentan-2-one, and sodium hydroxide were purchased from POCh (Gliwice, Poland). BMA was obtained in our laboratory according to the procedures described earlier [58].

### 2.2. Microspheres Synthesis

In our previous studies [52], we used quite a high amount of PVA to prevent of agglomeration of the synthesized microspheres and obtain a required diameter of the final beads. However, this approach led to some problems with the entire removal of the stabilizer from the porous surface of the product. Consequently, in the presented study, we conducted preliminary research focused on well-adjusted quantity of the stabilizer. The weight percentage of PVA in water was increased from 0.1 to 2.5 wt.%. It came out that application of a low PVA concentration resulted in agglomerated microspheres (Figure 1a). In the case of BMA copolymers, 1.5 wt.% of PVA turned to be sufficient for protection of the resulting microspheres and therefore this amount of stabilizer was used in further synthesis.

It was stirred with water in a three-necked flask for 6 h at 80 °C. After dissolving PVA, the organic solution of 15 g of the monomers (BMA with addition of a given comonomer), 0.075 g of an initiator (AIBN), and 22.5 mL of the diluent (toluene or chlorobenzene) was made and slowly put into the stirred aqueous medium. The molar ratio of DMA to a comonomer was kept 1:1 in the first series of synthesis; in the second, the molar ratio was 1:4. In order to obtain copolymers with highly developed internal structure, toluene and chlorobenzene were used as pore-forming diluents. The copolymerization process continued for 20 h at 80 °C. Porous microspheres obtained in this process were collected, filtered, washed with hot water and subjected to an intensive cleaning procedure described by Tuncel [59]. However, even this careful cleaning was not sufficient for complete removal of the stabilizer (Figure 1b). The purified copolymers were dried in a vacuum exsiccator at 60 °C. Table 1 delivers the designations of the obtained copolymers along with the main experimental parameters.

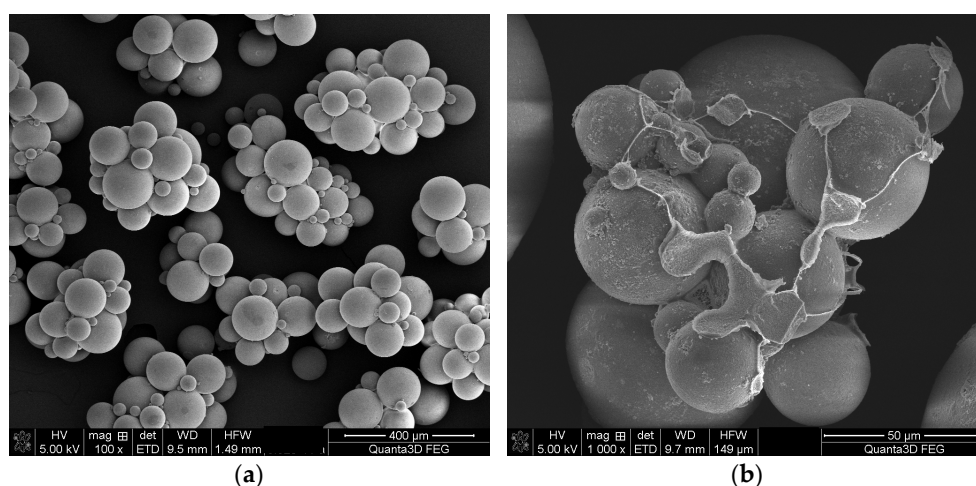


**Figure 1.** SEM image of BMA-co-TRIM\_C microspheres synthesized in the presence of 0.5 wt.% (a) and 2.5 wt.% (b) of PVA.

**Table 1.** The main experimental parameters of the microsphere synthesis.

Copolymer	Monomers	Monomers Ratio	Diluents (mL)		
			Toluene	Chlorobenzene	
BMA-co-EGDMA_1_T	BMA	EGDMA	1:1	22.5	-
BMA-co-EGDMA_1_C		EGDMA	1:1	22.5	22.5
BMA-co-EGDMA_4_T		EGDMA	1:4	22.5	-
BMA-co-EGDMA_4_C		EGDMA	1:4	22.5	22.5
BMA-co-DVB_1_T		DVB	1:1	22.5	-
BMA-co-DVB_1_C		DVB	1:1	22.5	22.5
BMA-co-DVB_4_T		DVB	1:4	22.5	-
BMA-co-DVB_4_C		DVB	1:4	22.5	22.5
BMA-co-TRIM_1_T	TRIM	TRIM	1:1	22.5	-
BMA-co-TRIM_1_C		TRIM	1:1	22.5	22.5
BMA-co-TRIM_4_T		TRIM	1:4	22.5	-
BMA-co-TRIM_4_C		TRIM	1:4	22.5	22.5

### 2.3. Measurement Methods

Structural characterization of the obtained materials was made on the basis of FTIR spectroscopy. For this purpose, a Bruker Tensor 27 FTIR spectrometer (Ettlingen, Germany) operating in the spectral range 4000–600  $\text{cm}^{-1}$  was used. The ATR-FTIR spectra were recorded with a resolution of 4  $\text{cm}^{-1}$ .

Porous structure of the investigated copolymers was ascertain based on the nitrogen amount adsorbed on the copolymers surface. The isotherms of nitrogen adsorption/desorption were collected at  $-196\text{ }^{\circ}\text{C}$  using ASAP 2405N analyzer (Micromeritics Corp., Norcross, GA, USA). Before the porous structure measurements, the copolymers were outgassed ( $10^{-2}$  mm Hg) at  $140\text{ }^{\circ}\text{C}$  for 2 h. The linear Brunauer–Emmet–Teller (BET) plots were applied to calculate the specific surface area ( $S_{BET}$ ). The pore volume ( $V$ ) was evaluated based on a single point adsorption at a relative pressure  $p/p_0 = 0.985$ . Pore size distributions (PSD) and its maxima ( $\text{PSD}_{\text{max}}$ ) was appraised according to the Barrett, Joyner and Halenda (BJH) approach [60]. The pore diameters ( $D_{BJH}$ ) were evaluated on the basis of the  $\text{PSD}_{\text{max}}$ .

A scanning electron microscope (SEM) Duall Beam<sup>TM</sup>, Quanta3D FEG (Fei Company, Hillsboro, OR, USA) was used for taking the images of the obtained microspheres. Their size and size distribution were measured by a Mastersizer Analyser 2000 (Malvern, Instruments Ltd., Worcestershire, UK). The British standard BS2955:1993 was the base for calculation of the distribution statistics. According to the standard,  $D(0.1)$  is the particle size below which 10% of the sample lies, whereas  $D(0.9)$  is the particle size below which 90% of the sample lies.  $D(0.5)$  refers to Mass Median Diameters (MMD) that is the size at which 50% of the sample is smaller and 50% is larger. All of the particle diameters are given in microns. Span (width of the size distribution) was calculated on the basis of the following formula:

$$\text{span} = \frac{D(0.9) - D(0.1)}{D(0.5)} \quad (1)$$

Thermogravimetric (TG) analyses were performed using a Netzsch STA 449 F1 Jupiter thermal analyzer (Selb, Germany) both in helium as well as synthetic air atmosphere (flow = 20 mL/min). The analysis temperature range was  $35\text{--}800\text{ }^{\circ}\text{C}$  whereas the heating rate was  $10\text{ }^{\circ}\text{C min}^{-1}$ . The measurements were performed in  $\text{Al}_2\text{O}_3$  crucibles. As a reference, an empty  $\text{Al}_2\text{O}_3$  (mass of  $\sim 160$  mg) crucible was used. The sample masses were about 10 mg. On the basis of the TG curves, the characteristic temperatures of  $T_{5\%}$ ,  $T_{20\%}$ ,  $T_{50\%}$  mass losses as well as final decomposition temperature ( $FDT$ ) were determined. In turn, on the basis of differential TG (DTG) curves, the temperature of the maximum rate of mass loss ( $T_{\text{max}}$ ) for individual decomposition stages was gauged.

Inverse gas chromatography (IGC) was applied for the determination of the polarity of the copolymers under study. To determine this parameters McReynolds procedure [55] was put to use. This method based on McReynolds' constants ( $\Delta I$ ) of test substances: benzene (x), butan-1-ol (y), pentan-2-one (z). The constants can be determined by computing the difference between the Kovats' index for benzene, butan-1-ol, pentan-2-one on the investigated stationary phase and graphitized thermally carbon black (GTCB). The overall polarity of the phase under study can be established by the sum of the McReynolds constant. The chromatographic measurements were performed Dani GC 1000 gas chromatograph (Milan, Italy) fitted with a thermal conductivity detector (TCD), an injector, and stainless-steel columns ( $100\text{ cm} \times 1.6\text{ mm I.D.}$ ) packed with the studied porous microspheres. The retention times for the test compounds were determined in helium at a flow-rate of 50 mL/min. A 1  $\mu\text{L}$  syringe (SGE, North Melbourne, Australia) was used for manual injection of the samples. The measurements temperature was kept isothermally at  $140\text{ }^{\circ}\text{C}$ .

### 3. Results

In the synthesis of permanently porous microspheres, a suspension polymerization technique was used. Compared to previous studies, we have significantly reduced the amount of the used PVA, still obtaining regular microspheres. In their synthesis, three commercially available monomers were copolymerized with 9,10-bis(methacryloyloxymethyl) anthracene. The chemical structures of the monomers used in the synthesis of porous copolymers are displayed in Figure 2.

To settle the assumed chemical structure of the obtained microspheres, ATR-FTIR spectrophotometry was applied. The obtained spectra of the copolymers under study are

displayed on Figure 3. As the copolymers exhibit some analogous functional groups, bands pointing the presence of aromatic rings, i.e., at  $3066\text{--}3019\text{ cm}^{-1}$  ( $\nu$  C-H),  $1603\text{ cm}^{-1}$  and  $1458\text{ cm}^{-1}$  ( $\nu$  C-C), ester groups at  $1726\text{ cm}^{-1}$  ( $\nu$  C=O) and  $1249\text{--}1139\text{ cm}^{-1}$  ( $\nu$  C-O) as well as alkyl and alkylene groups, i.e., at  $2962\text{--}2830\text{ cm}^{-1}$  ( $\nu$  asym. and sym. C-H) are visible on each spectrum. A weak absorption band at  $1638\text{--}1630\text{ cm}^{-1}$  connected with the unreacted C=C double bonds can be also seen in some spectra. In the case of BMA-co-DVB copolymers, bands at  $755$  and  $708\text{ cm}^{-1}$  ( $\delta$  oop C-H of monosubstituted benzene) and at  $829\text{--}796\text{ cm}^{-1}$  ( $\delta$  out-of-plane C-H of *p*-disubstituted benzene) are also visible.

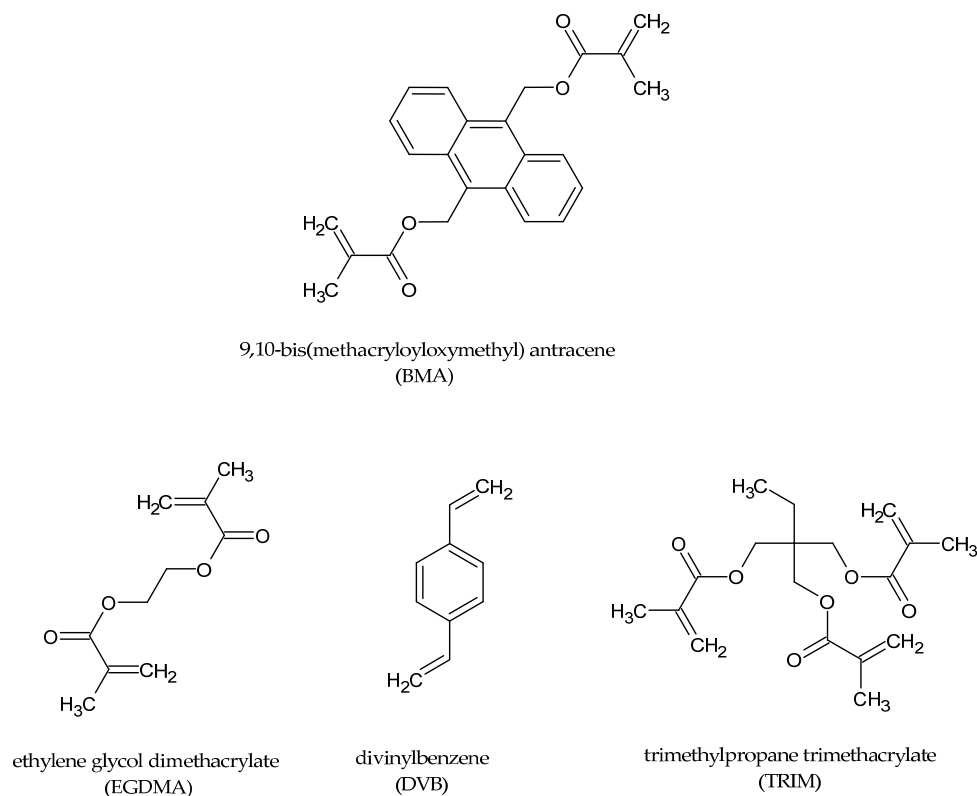


**Figure 2.** The chemical formulas of the used monomers.

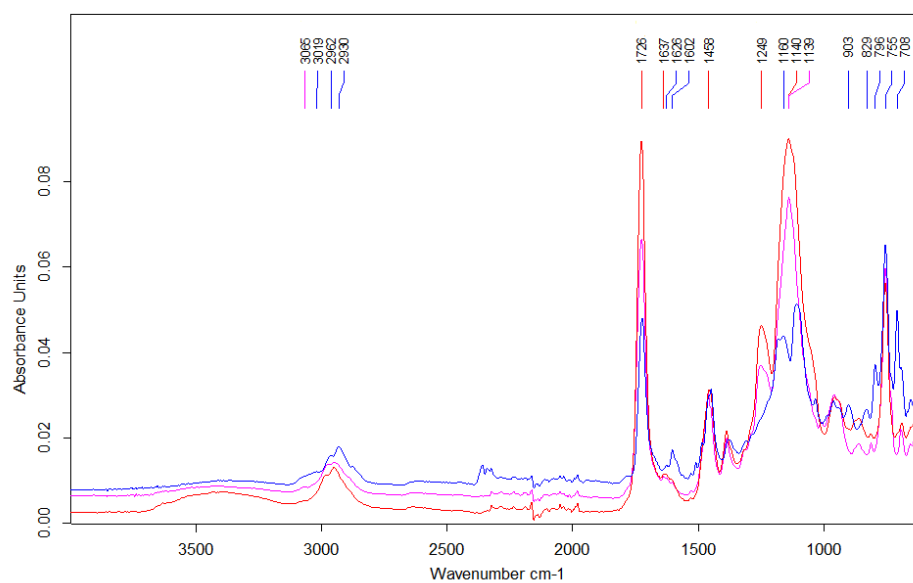


**Figure 3.** ATR-FTIR spectra of BMA-co-DVB (blue line), BMA-co-EGDMA (pink line) and BMA-co-TRIM (red line) copolymers.

The premediated objective of this research was to synthesize new polymeric materials with highly developed internal structure. In order to obtain this goal, BMA with different methacrylic and vinyl comonomers was polymerized in the presence of two different solvents. All of the used comonomers possess a high functionality, which leads to the high degree of crosslinking. The functionality of EGDMA and DVB is the same as that of BMA and is equal to four. It is even higher and equals six in the case of TRIM. This fact creates an excellent environment for  $\nu$ -syneresis.

As evidenced in Table 2, the increase in monomer functionality expands the porous structure. BMA-co-TRIM copolymers have the highly developed internal structure. This phenomenon is reflected by high value of specific surface area, pore volume and diversified pore size distribution. What is important, not only is the type of comonomer important for the process of porous structure formation, but also its amount. In the first turn, the copolymers were synthesized using equimolar rations. Afterwards, the amount of the comonomer (EGDMA, DVB or TRIM) was increased and the molar ratio of BMA to comonomer was equal to 1:4. The increase in the comonomer amount in the polymerization medium gave rise to creation of a huge number of low energy and highly crosslinked nuclei during the phase separation. After the nuclei aggregation, the resulting microgels are very complex and create highly developed internal structure. The value of the specific surface area of copolymers obtained with the comonomer excess is considerably higher compared with their equimolar counterparts. A similar relationship can be observed with the pore volume. The chemical structure of the comonomer also has a great impact on the pore diameter. Figure 4 displays pore size distribution of microspheres obtained from equimolar amount of comonomers with toluene as porogenic solvent. As can be seen, the pore diameters strongly depend on the used comonomer. BMA-co-DVB copolymers are characterized by narrow pore size distribution and pore diameters approaching the micropore region. In the case of BMA-co-TRIM materials, the distribution is wider and apart from a small peak at 3.5 nm the maximum pore diameter is observed at 15 nm. The copolymers obtained on the basis of EGDMA possesses larger pores. Their size distribution is shifted towards macropores, and the maximum can be seen at 40 nm. The same pattern can be noted for the copolymers with molar ratio of comonomers equals to 1:4. The pores are slightly smaller, but the described tendency is preserved. What is important, the reduced diameter of the pores contributes to more developed internal structure (Table 2). What is more, the application of chlorobenzene in the synthesis of porous copolymers gave rise to further increases in the main parameters characterizing the porous structure. This phenomenon is connected with the better solvation power of chlorobenzene compared with toluene. Its Hildebrand solubility parameter is equal to 19.6 (MPa)<sup>0.5</sup> whereas this of toluene is 18.2 (MPa)<sup>0.5</sup>.

**Table 2.** Parameters characterizing porous structure of the copolymeric microspheres.

Copolymer	Specific Surface Area $S_{BET}$ (m <sup>2</sup> /g)	Pore Volume $V$ (cm <sup>3</sup> /g)	Pore Diameter $D_{BJH}$ (nm)
BMA-co-EGDMA_1_T	134.30 ± 0.34	0.1641 ± 0.0012	40
BMA-co-EGDMA_1_C	220.49 ± 0.36	0.6299 ± 0.0009	3.9
BMA-co-EGDMA_4_T	220.91 ± 0.48	0.5953 ± 0.0021	37
BMA-co-EGDMA_4_C	411.94 ± 0.99	0.6410 ± 0.0005	4.1/11 *
BMA-co-DVB_1_T	252.32 ± 0.64	0.2028 ± 0.0011	3.5
BMA-co-DVB_1_C	384.28 ± 0.14	0.4099 ± 0.0008	4
BMA-co-DVB_4_T	358.13 ± 0.57	0.2398 ± 0.0009	2.5
BMA-co-DVB_4_C	412.34 ± 0.71	0.4110 ± 0.0015	4.8/17 *
BMA-co-TRIM_1_T	265.46 ± 0.42	0.3327 ± 0.0036	3.6/15 *
BMA-co-TRIM_1_C	440.34 ± 0.31	0.7309 ± 0.0004	3.5/12 *
BMA-co-TRIM_4_T	335.93 ± 0.44	0.4618 ± 0.0022	10
BMA-co-TRIM_4_C	472.36 ± 0.29	0.7498 ± 0.0007	8.5

\* bimodal pore size distribution.

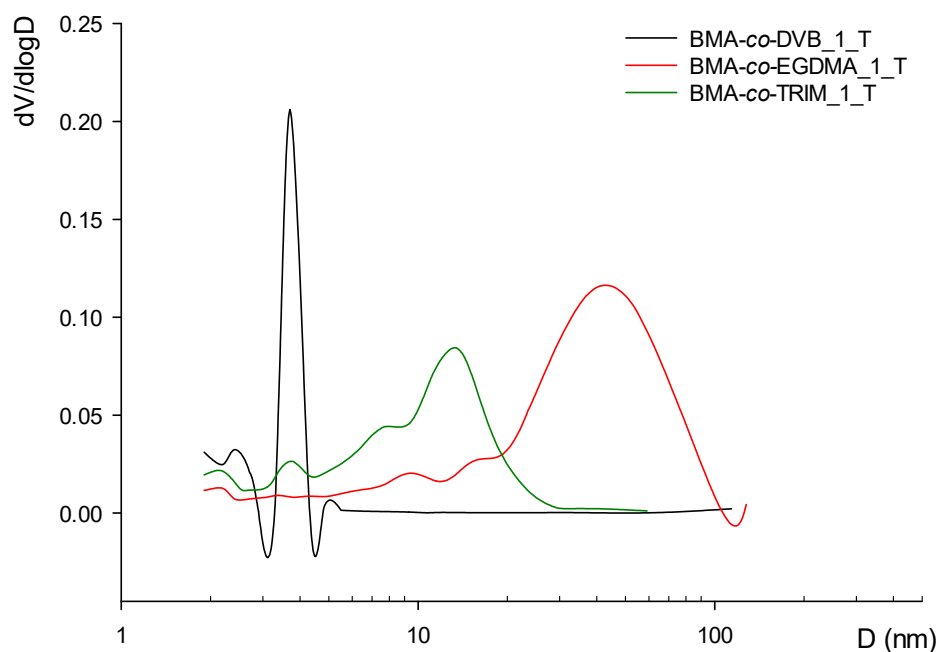


**Figure 4.** Pore size distribution for selected copolymers.

Generally, the formation of porous materials was possible thanks to the application of the suspension technique in the synthesis. The characteristic feature of the suspension technique is the fact that the size and size distribution of the obtained microspheres depends on many polymerization factors (the diameter of a stirrer and a flask, the volume ratio of the water phase to the organic phase, the mixing power and the stabilizer concentration) [61]. Due to the chemical diversity of monomers, differences in organic phase densities were observed, and consequently, different interfacial tension was present. This phenomenon was evident in the synthesized microspheres size. The mass median diameter of BMA-co-DVB copolymers did not exceed 100  $\mu\text{m}$ . The use of methacrylate comonomers results in microspheres of larger size. The diameters of BMA-co-EGDMA copolymers are in the range 89–184  $\mu\text{m}$ , whereas BMA-co-TRIM copolymers in the range 76–217  $\mu\text{m}$  depending on the molar ratio of the monomers and the used solvent. The detailed data of particle size and particle size distribution are collected in Table 3.

**Table 3.** The statistical data of particle size distribution.

Copolymeric Microsphere	$D(0.1)$ ( $\mu\text{m}$ )	$D(0.5)$ ( $\mu\text{m}$ )	$D(0.9)$ ( $\mu\text{m}$ )	Span
BMA-co-EGDMA_1_T	94	132	164	0.530
BMA-co-EGDMA_1_C	98	141	179	0.574
BMA-co-EGDMA_4_T	89	138	171	0.592
BMA-co-EGDMA_4_C	101	147	184	0.565
BMA-co-DVB_1_T	68	95	101	0.347
BMA-co-DVB_1_C	70	97	128	0.598
BMA-co-DVB_4_T	64	92	114	0.543
BMA-co-DVB_4_C	73	100	136	0.624
BMA-co-TRIM_1_T	80	162	181	0.623
BMA-co-TRIM_1_C	98	174	201	0.592
BMA-co-TRIM_4_T	76	168	196	0.714
BMA-co-TRIM_4_C	102	183	217	0.628

The referred differences are also clearly visible in Figure 5. The SEM images show the regular shape of the synthesized microspheres and confirm the data obtained using laser diffraction.

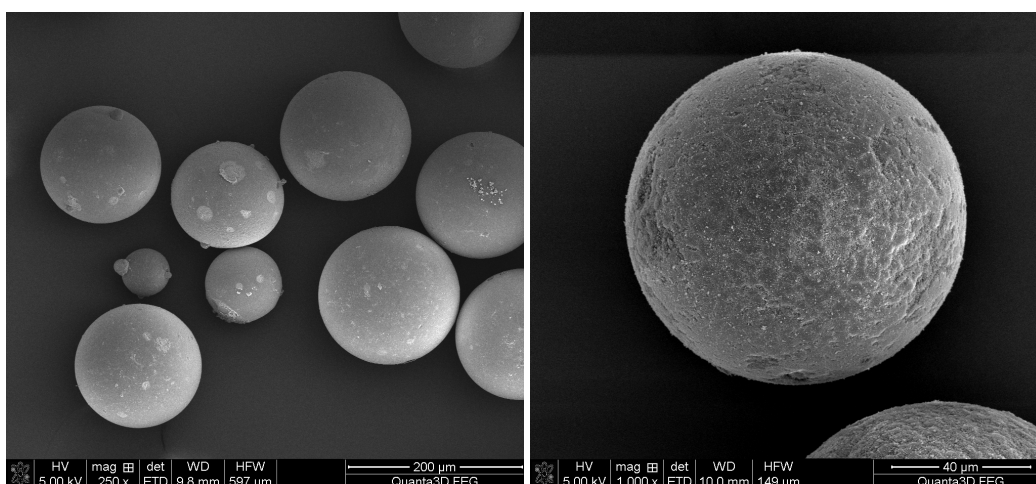


**Figure 5.** SEM images of the BMA-co-DVB\_1\_T (left) and BMA-co-TRIM\_1\_T (right) copolymers.

One of the most important characteristics of polymeric materials is their thermal resistance. In this study, thermal properties of the investigated copolymers were evaluated on the basis of thermogravimetry. Based on TG studies, it can be concluded that all of the copolymer under study exhibit good thermal stability in inert as well as oxidative atmospheres (Tables 4 and 5). Among them, the best thermal resistance demonstrated BMA-co-TRIM copolymers. Its initial decomposition temperature was above 300 °C. This phenomenon is caused by the high (equal six) functionality of TRIM and its possibility to form highly crosslinked polymeric network. On the other hand, the value of final decomposition temperature was observed for BMA-co-DVB copolymers. The chemical structure of the DVB monomer can explain this fact. It possesses an aromatic ring that contributes to better thermal stability. Increasing the molar ratio to 1:4 for DVB as well as for TRIM resulted in the enhancement of thermal resistance of the synthesized copolymers. The opposite relationship was observed for EGDMA. Generally, the least thermally stable are copolymers of this tetrafunctional, aliphatic comonomer. All the indicators of thermal resistance determined for BMA-co-EGDMA microspheres have the lowest value among all investigated materials.

**Table 4.** The characteristic temperatures determined on the basis of TG and DTG data (helium atmosphere).

Copolymeric Microspheres	$T_{5\%}$ (°C)	$T_{20\%}$ (°C)	$T_{50\%}$ (°C)	$T_{max1}$ (°C)	$T_{max2}$ (°C)	$T_{max2}$ (°C)	FDT
BMA-co-DVB_1	256	307	367	335	425	646	720
BMA-co-DVB_4	261	312	381	343	431	658	738
BMA-co-EGDMA_1	254	301	356	320	417	571	673
BMA-co-EGDMA_4	241	286	341	311	402	562	664
BMA-co-TRIM_1	304	346	434	325	442	571	680
BMA-co-TRIM_4	309	358	452	336	456	583	692

**Table 5.** The characteristic temperatures determined on the basis of TG and DTG (synthetic air atmosphere).

Copolymeric Microspheres	$T_{5\%}$ (°C)	$T_{20\%}$ (°C)	$T_{50\%}$ (°C)	$T_{max1}$ (°C)	$T_{max2}$ (°C)	$T_{max3}$ (°C)	FDT
BMA-co-DVB_1	251	316	367	360	421	626	701
BMA-co-DVB_4	258	318	374	368	429	641	718
BMA-co-EGDMA_1	250	303	339	310	414	536	591
BMA-co-EGDMA_4	243	298	327	302	408	528	583
BMA-co-TRIM_1	301	327	369	335	456	536	596
BMA-co-TRIM_4	307	331	374	339	461	542	601

What is worth noticing, thermal decomposition in helium atmosphere of all investigated copolymers proceeded in three, partially superimposed steps (Figure 6).

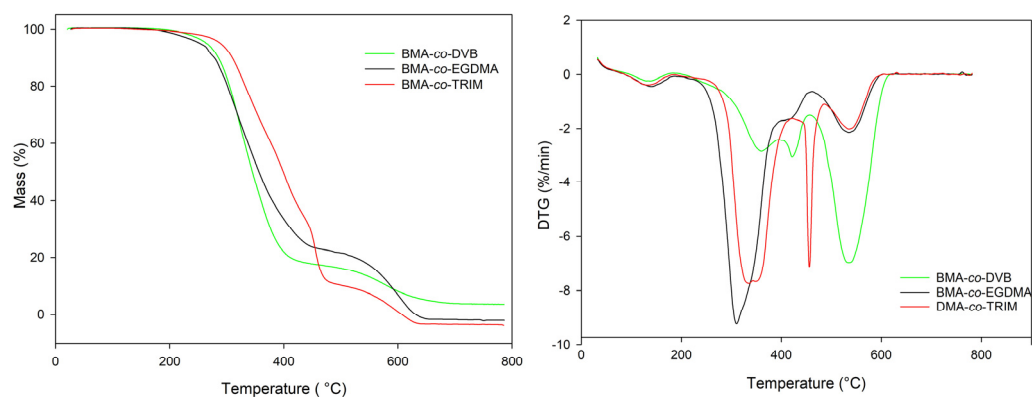


**Figure 6.** TG (left) and DTG (right) curves of the investigated copolymers obtained in helium.

In the case of synthetic air, all the main indicators of thermal resistance possess lower values compared with their counterparts determined in helium. The oxidative atmosphere accelerates the thermal decomposition of the investigated microspheres and the went in three main stages (Figure 7) with the maxima from 302 to 461 °C. The noises that happened in the plots are associated with the high sensitivity of the thermal analyzer. They occurred at the end of measurements and did not have relevant impact on the acquired results.

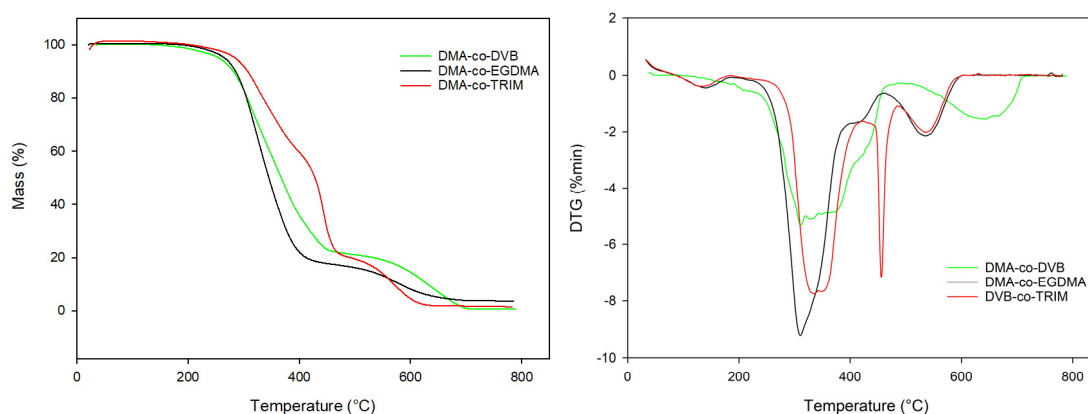


**Figure 7.** TG (left) and DTG (right) curves of the investigated copolymers obtained in synthetic air.

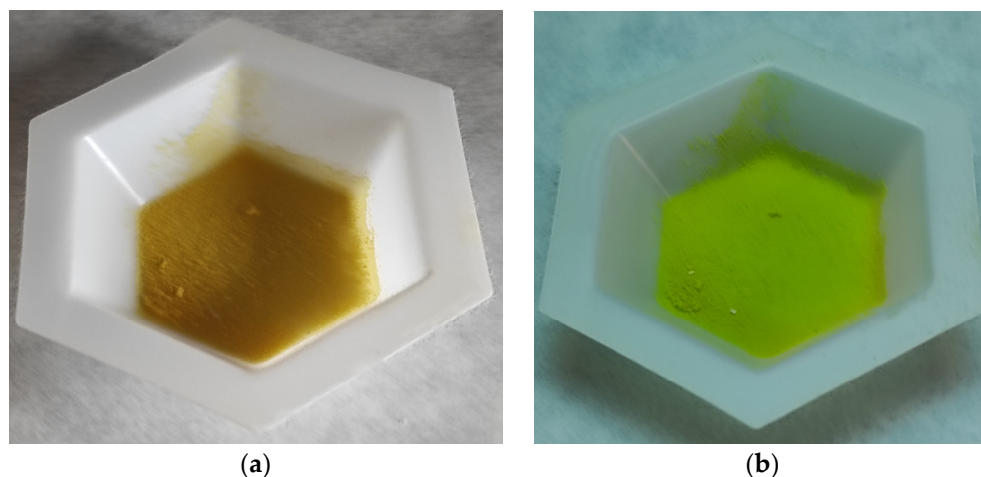
What is interesting, the type of porogen used in the synthesis did not have any impact on the thermal behavior. The copolymers obtained in the presence of chlorobenzene have almost identical value of characteristic temperatures as in the case of toluene.

The application of various monomers in the synthesis of polymeric microbeads results in different chemical characters of the surface. One of the suitable methods for investigation of surface character is inverse gas chromatography. Microspheres for gas chromatography should be thermally stable, quite rigid, and have a large interacting surface area. As all the studied copolymers fulfilled these requirements, it was possible to determine their polarity indexes and overall polarity ( $\Sigma\Delta I$ ) using this technique. A polarity index ranks adsorbents by the sum of McReynolds' constant of the test substances. Generally, the higher the polarity index, the more polar the adsorbent. Table 6 presents Kovats' retention indices for the McReynolds' test substances determined at 140 °C. The lowest value of  $\Sigma\Delta I$ , e.g., 441 was observed for BMA-co-DVB copolymer. This is a higher value compared to the one of ST-co-DVB copolymer determined in analogical way in our previous study [52]. The replacement of DVB by methacrylate comonomers causes a considerable increase in overall polarity. EGDMA and TRIM have the same functional group. As a consequence, the  $\Sigma\Delta I$  is almost identical for both BMA-co-EGDMA and BMA-co-TRIM copolymers.

**Table 6.** Kovats' retention indices for the McReynolds' test substances and overall polarity ( $\Sigma\Delta I$ ) for the porous copolymers.

Copolymeric Microsphere	Kovats' Retention Indices			McReynolds' Constants			
	$I_x$ (Benzene)	$I_y$ (Butan-1-ol)	$I_z$ (Pentan-2-one)	$\Delta I_x$	$\Delta I_y$	$\Delta I_z$	$\Sigma\Delta I$
BMA-co-DVB_1	649	698	718	75	210	156	441
BMA-co-EGDMA_1	673	753	749	99	264	184	547
BMA-co-TRIM_1	669	748	759	95	259	194	548
GTCB	574	489	565	-	-	-	-

In the last stage of the investigation, the obtained copolymers were subjected to ultraviolet radiation. It turned out that they exhibit fluorescence under UV light (Figure 8). This phenomenon is associated with the presence of anthracene rings in the structure of the porous copolymers.

**Figure 8.** The images of the BMA-co-TRIM\_4\_T copolymer (a) before and (b) under UV radiation.

#### 4. Conclusions

The main aim of the presented paper was synthesis and characterization porous, chemically diversified, thermally stable polymeric microspheres. To achieve this goal, BMA was used as functional monomer whereas DVB, EGDMA and TRIM served mainly as crosslinkers. The application of suspension polymerization allowed for the creation of porous, highly crosslinked materials. It was found out that in the case of BMA copolymers, 1.5 wt.% of suspension stabilizer is required to obtain the product in the form of regular microspheres. The porous structure of the obtained microbeads strongly depends on the used comonomer and porogen type. The most developed internal structure possesses BMA-co-TRIM\_4 copolymer synthesized in the presence of chlorobenzene as a pore-forming diluent. The incorporation of anthracene rings in the copolymers structure as well as high degree of crosslinking contributes to very good thermal stability in oxidative and inert atmosphere. The presence of different functional groups on the surface is responsible for different kind of interaction when the microspheres serve as adsorbents what was evidenced via inverse gas chromatography. What is interesting, the obtained porous copolymers exhibit fluorescence under UV light. They can be potentially applied as precursor for thermally resistant sensors and this direction is going to be the subject of our further investigation.

**Author Contributions:** Conceptualization, M.M.; methodology, M.M.; formal analysis, M.M. and M.J.; investigation, M.M. and M.J.; writing—original draft preparation, M.M. and M.J.; writing—review and editing, M.M. and M.J. All authors have read and agreed to the published version of the manuscript.

**Funding:** This research received no external funding.

**Institutional Review Board Statement:** Not applicable.

**Informed Consent Statement:** Not applicable.

**Data Availability Statement:** The data presented in this study are available on request from the corresponding authors.

**Conflicts of Interest:** The authors declare no conflict of interest.

## References

1. Grochowicz, M. Poly(glycidyl methacrylate-co-1,4-dimethacryloyloxybenzene) monodisperse microspheres—Synthesis, characterization and application as chromatographic packings in RP-HPLC. *React. Funct. Polym.* **2019**, *137*, 1–10. [[CrossRef](#)]
2. Zhang, C.; Peng, Q.; Wang, S.; Guo, L.; Cong, H.; Shen, Y.; Yu, B. Preparation of poly (KH570-co-DVB) microspheres and application in HPLC for separation of benzene and benzene homologs. *Ferroelectrics* **2020**, *562*, 145–151. [[CrossRef](#)]
3. Kazakevich, Y.; Kant, M. Size-exclusion and the void volume of HPLC column. *J. Liq. Chromatogr. Relat.* **2019**, *42*, 89–98. [[CrossRef](#)]
4. Bai, J.; Zhu, Q.; Tang, C.; Liu, J.; Yi, Y.; Bai, Q. Synthesis and application of 5  $\mu\text{m}$  monodisperse porous silica microspheres with controllable pore size using polymeric microspheres as templates for the separation of small solutes and proteins by high-performance liquid chromatography. *J. Chromatogr. A* **2022**, *1675*, 463165. [[CrossRef](#)] [[PubMed](#)]
5. Pączkowski, P.; Gawdzik, B. Studies on Preparation, Characterization and Application of Porous Functionalized Glycidyl Methacrylate-Based Microspheres. *Materials* **2021**, *14*, 1438. [[CrossRef](#)] [[PubMed](#)]
6. Smigol, A.V.; Svec, F. Synthesis and properties of uniform beads based on macroporous copolymer glycidyl methacrylate–ethylene dimethacrylate: A way to improve separation media for HPLC. *J. Appl. Polym. Sci.* **1992**, *46*, 1439–1448. [[CrossRef](#)]
7. Ellingsen, T.; Aune, O.; Ugelstad, J.; Hagen, S. Monosized stationary phases for chromatography. *J. Chromatogr.* **1990**, *535*, 147–161. [[CrossRef](#)]
8. Galia, M.; Svec, F.; Frechet, J.M.J. Monodisperse polymer beads as packing material for high-performance liquid chromatography: Effect of divinylbenzene content on the porous and chromatographic properties of poly(styrene-co-divinylbenzene) beads prepared in presence of linear polystyrene as a porogen. *J. Polym. Sci. A Polym. Chem.* **1994**, *32*, 2169–2175.
9. Unsal, E.; Elmas, B.; Çamlı, S.T.; Tuncel, M.; Şenel, S.; Tuncel, A. Monodisperse-porous poly(styrene-co-divinylbenzene) beads providing high column efficiency in reversed phase HPLC. *J. Appl. Polym. Sci.* **2005**, *95*, 1430–1438. [[CrossRef](#)]
10. Müller, A.; Xu, Z.; Greiner, A. Preparation and Performance Assessment of Low-Pressure Affinity Membranes Based on Functionalized, Electrospun Polyacrylates for Gold Nanoparticle Filtration. *Appl. Mater. Interfaces* **2021**, *13*, 15659–15667. [[CrossRef](#)]
11. George, J.; Kumar, V.V. Designing a novel poly (methyl vinyl ether maleic anhydride) based polymeric membrane with enhanced antifouling performance for removal of pentachlorophenol from aqueous solution. *Environ. Res.* **2023**, *223*, 115404. [[CrossRef](#)] [[PubMed](#)]
12. Xie, Z.; Wang, C.; deKrafft, K.E.; Lin, W. Highly Stable and Porous Cross-Linked Polymers for Efficient Photocatalysis. *J. Am. Chem. Soc.* **2011**, *133*, 2056–2059. [[CrossRef](#)]
13. Guo, X.; Zhang, F.; Muhammad, Y.; Cai, Z.; Gao, L.; Wei, R.; Xiao, G. Functional porous poly(ionic liquid)s catalyst for highly integrated capture and conversion of flue gas CO<sub>2</sub>. *Fuel* **2023**, *339*, 126913. [[CrossRef](#)]
14. Moslan, M.S.; Othman, M.; Samavati, A.; Theodosiou, A.; Kalli, K.; Ismail, A.; Rahman, M.A. Real-time fluid flow movement identification in porous media for reservoir monitoring application using polycarbonate optical fibre bragg grating sensor. *Sens. Actuator A Phys.* **2023**, *354*, 114246. [[CrossRef](#)]
15. Wang, K.; Wen, H.F.; Yu, D.G.; Yang, Y.; Zhang, D.F. Electrospayed hydrophilic nanocomposites coated with shellac for colon-specific delayed drug delivery. *Mater. Des.* **2018**, *143*, 248–255. [[CrossRef](#)]
16. Yang, Y.; Liu, Z.P.; Yu, D.G.; Wang, K.; Liu, P.; Chen, X. Colon-specific pulsatile drug release provided by electrospun shellac nanocoating on hydrophilic amorphous composites. *Int. J. Nanomed.* **2018**, *13*, 2395–2404. [[CrossRef](#)]
17. Chen, H.; Zhang, L.; Li, M.; Xie, G. Synthesis of Core–Shell Micro/Nanoparticles and Their Tribological Application: A Review. *Materials* **2020**, *13*, 4590. [[CrossRef](#)]
18. Wawrzkievicz, M.; Podkoscielna, B.; Podkoscielny, P. Application of functionalized DVB-co-GMA polymeric microspheres in the enhanced sorption process of hazardous dyes from dyeing baths. *Molecules* **2020**, *25*, 5247. [[CrossRef](#)] [[PubMed](#)]
19. Podkoscielna, B.; Wawrzkievicz, M.; Klapiszewski, Ł. Synthesis, Characterization and Sorption Ability of Epoxy Resin-Based Sorbents with Amine Groups. *Polymers* **2021**, *13*, 4139. [[CrossRef](#)] [[PubMed](#)]
20. Mane, S.; Li, Y.; Xue, D.; Liu, X.; Sun, L. Rational design and fabrication of nitrogen-enriched and hierarchical porous polymers targeted for selective carbon capture. *Ind. Eng. Chem. Res.* **2018**, *57*, 12926–12934. [[CrossRef](#)]
21. Hamdy, L.B.; Wakeham, R.J.; Taddei, M.; Barron, A.R.; Andreoli, E. Epoxy Cross-Linked Polyamine CO<sub>2</sub> Sorbents Enhanced via Hydrophobic Functionalization. *Chem. Mater.* **2019**, *31*, 4673–4684. [[CrossRef](#)]
22. Brewer, A.; Florek, J.; Kleitz, F. A perspective on developing solid-phase extraction technologies for industrial-scale critical materials recovery. *Green Chem.* **2022**, *24*, 2752–2765. [[CrossRef](#)] [[PubMed](#)]

23. Grochowicz, M.; Szajnecki, Ł.; Rogulska, M. Crosslinked 4-vinylpyridine monodisperse functional microspheres for sorption of ibuprofen and ketoprofen. *Polymers* **2022**, *14*, 2080. [[CrossRef](#)] [[PubMed](#)]
24. Ghosh, S.; Acharyya, M. Design of novolac resin-based network polymers for adsorptive removal of azo dye molecules. *RSC Adv.* **2016**, *6*, 28781–28786. [[CrossRef](#)]
25. Ali, F.; Shah, Z.; Khan, A.; Saadia, M.; AlOthman, Z.A.; Cheong, W.J. Synthesis, column packing and liquid chromatography of molecularly imprinted polymers for the acid black 1, acid black 210, and acid brown 703 dyes. *RSC Adv.* **2022**, *12*, 19611–19623. [[CrossRef](#)]
26. Yi, F.; Xie, W.; Li, H.; Zeng, L.; Li, W.; Lei, F. Preparation of core-shell SiO<sub>2</sub>@Rosin-based polymer high performance liquid preparation column and purification of camptothecin. *Chem. Ind. For. Prod.* **2021**, *41*, 67–75.
27. Gritti, F.; Nawada, S. On the road toward highly efficient and large volume three-dimensional-printed liquid chromatography columns. *J. Sep. Sci.* **2022**, *45*, 3232–3240. [[CrossRef](#)]
28. Pang, L.; Xue, T.; Cong, H.; Shen, Y.; Yu, B. Preparation and application of PGMA-DVB microspheres via surface-modification with quaternary and phenylboronic acid moiety. *Colloids Surf. B Biointerfaces* **2020**, *188*, 110807. [[CrossRef](#)]
29. Michálek, J.; Dušková Smrčková, M.; Příkladný, M.; Chylíková Krumbholcová, E.V.A. Story of a material, or 2-hydroxyethyl methacrylate: Monomer, polymer, properties and uses. *Chemické Listy* **2018**, *112*, 490–497.
30. Auerbach, S.; Carrado, K.; Dutta, P. (Eds.) *Handbook of Zeolite Science and Technology*; CRC Press: Boca Raton, FL, USA, 2003; ISBN 9780824740207.
31. Kambarova, E.A.; Gavrilenko, M.A.; Bektenov, N.A. Zeolites modified with polyethylene polyamine and epoxy resin to extract lead ions from wastewater. *Bull. Tomsk Polytech. Univ. Geo Assets Eng.* **2021**, *332*, 7–13.
32. Qian, J.; Zhang, W.; Yang, X.; Yan, K.; Shen, M.; Pan, H.; Wang, L. Tailoring zeolite ERI aperture for efficient separation of CO<sub>2</sub> from gas mixtures. *Sep. Purif. Technol.* **2023**, *309*, 123078. [[CrossRef](#)]
33. Chmielarz, L.; Kowalczyk, A.; Skoczek, M.; Rutkowska, M.; Gil, B.; Natkański, P.; Ryczkowski, J. Porous clay heterostructures intercalated with multicomponent pillars as catalysts for dehydration of alcohols. *Appl. Clay Sci.* **2018**, *160*, 116–125. [[CrossRef](#)]
34. Cecilia, J.A.; García-Sancho, C.; Vilarrasa-García, E.; Jiménez-Jiménez, J.; Rodríguez-Castellón, E. Synthesis, Characterization, Uses and Applications of Porous Clays Heterostructures: A Review. *Chem. Rec.* **2018**, *18*, 1085–1104. [[CrossRef](#)]
35. Vilarrasa-García, E.; Cecilia, J.A.; Azevedo, D.; Cavalcante, C.; Rodríguez-Castellón, E. Evaluation of porous clay heterostructures modified with amine species as adsorbent for the CO<sub>2</sub> capture. *Micropor. Mesopor. Mat.* **2017**, *249*, 25–33. [[CrossRef](#)]
36. Zhang, T.; Wang, W.; Zhao, Y.; Bai, H.; Wen, T.; Kang, S.; Komarneni, S. Removal of heavy metals and dyes by clay-based adsorbents: From natural clays to 1D and 2D nano-composites. *Chem. Eng. J.* **2021**, *420*, 127574. [[CrossRef](#)]
37. Allen, S.; Murray, M.; Brown, P.; Flynn, O. Peat as an adsorbent for dyestuffs and metals in wastewater. *Res. Cons. Rec.* **1994**, *11*, 25–39. [[CrossRef](#)]
38. Alsaman, A.S.; Ahmed, M.S.; Ibrahim, E.M.M.; Ali, E.S.; Farid, A.M.; Askalany, A.A. Experimental investigation of porous carbon for cooling and desalination applications. *Npj Clean Water* **2023**, *6*, 4. [[CrossRef](#)]
39. Priya, D.S.; Kennedy, L.J.; Anand, G.T. Emerging trends in biomass-derived porous carbon materials for energy storage application: A critical review. *Mater. Today Sustain.* **2023**, *21*, 100320. [[CrossRef](#)]
40. Wu, Y.; Weckhuysen, B.M. Separation and purification of hydrocarbons with porous materials. *Angew. Chem. Int. Ed. Engl.* **2021**, *60*, 18930–18949. [[CrossRef](#)]
41. Andrade, L.S.; Lima, H.; Silva, C.; Amorim, W.; Poço, J.; López-Castillo, A.; Mandelli, D. Metal–organic frameworks as catalysts and biocatalysts for methane oxidation: The current state of the art. *Coord. Chem. Rev.* **2023**, *481*, 215042. [[CrossRef](#)]
42. Xu, W.; Thapa, K.B.; Ju, Q.; Fang, Z.; Huang, W. Heterogeneous catalysts based on mesoporous metal–organic frameworks. *Coord. Chem. Rev.* **2018**, *373*, 199–232. [[CrossRef](#)]
43. Liu, Z.; Lu, Y.; Wang, C.; Zhang, Y.; Jin, X.; Wu, J.; Wu, C. MOF-derived nano CaO for highly efficient CO<sub>2</sub> fast adsorption. *Fuel* **2023**, *340*, 127476. [[CrossRef](#)]
44. Verma, R.; Dhingra, G.; Malik, A.K. A comprehensive review on metal organic framework based preconcentration strategies for chromatographic analysis of organic pollutants. *Crit. Rev. Anal. Chem.* **2023**, *53*, 415–441. [[CrossRef](#)] [[PubMed](#)]
45. Wen, Y.; Zhang, J.; Xu, Q.; Wu, X.; Zhu, Q. Pore surface engineering of metal–organic frameworks for heterogeneous catalysis. *Coord. Chem. Rev.* **2018**, *376*, 248–276. [[CrossRef](#)]
46. Yang, Y.; Tan, B.; Wood, C.D. Solution-processable hypercrosslinked polymers by low cost strategies: A promising platform for gas storage and separation. *J. Mater. Chem. A* **2016**, *4*, 15072–15080. [[CrossRef](#)]
47. Wood, C.D.; Tan, B.; Trewin, A.; Su, F.; Rosseinsky, M.J.; Bradshaw, D.; Sun, Y.; Zhou, L.; Cooper, A.I. Microporous Organic Polymers for Methane Storage. *Adv. Mater.* **2008**, *20*, 1916–1921. [[CrossRef](#)]
48. Kaur, P.; Hupp, J.T.; Nguyen, S.T. Porous Organic Polymers in Catalysis: Opportunities and Challenges. *ACS Catal.* **2011**, *1*, 819–835. [[CrossRef](#)]
49. Maciejewska, M.; Grochowicz, M. Synthesis and thermal characterization of porous polymeric microspheres functionalized with thiol groups. *J. Therm. Anal. Calorim.* **2023**. [[CrossRef](#)]
50. Sobiesiak, M. Analysis of structure and properties of DVB–GMA based porous polymers. *Adsorption* **2019**, *25*, 257–266. [[CrossRef](#)]
51. Sing, K.; Everett, D.H.; Haul, R.A.; Moscou, L.; Pierotti, R.A.; Rouquerol, J.; Siemieniewska, T. Reporting Physisorption Data for Gas/Solid Systems with Special Reference to the Determination of Surface Area and Porosity. *Pure Appl. Chem.* **1985**, *57*, 603–619. [[CrossRef](#)]

52. Maciejewska, M.; Gawdzik, B.; Rogulska, M. Regular polymeric microspheres with highly developed internal structure and remarkable thermal stability. *Materials* **2021**, *14*, 2240. [[CrossRef](#)] [[PubMed](#)]
53. Collin, G.; Höke, H.; Talbiersky, J. "Anthracene" in *Ullmann's Encyclopedia of Industrial Chemistry*, 7th ed.; Wiley-VCH: Weinheim, Germany, 2011; ISBN 9783527303854.
54. Podkościelna, B. Synthesis, spectroscopic and thermal characterization of the new photoluminescent monomer 2,7-di(methacyloyloxy)naphthalene and its copolymerization with selected vinyl monomers. *J. Therm. Anal. Calorim.* **2016**, *123*, 273–282. [[CrossRef](#)]
55. Fila, K.; Podkościelna, B.; Podgórski, M. Cross-Linked Polythiomethacrylate Esters Based on Naphthalene—Synthesis, Properties and Reprocessing. *Materials* **2020**, *3*, 3021. [[CrossRef](#)]
56. Maciejewska, M.; Osypiuk-Tomasik, J. Sorption on porous copolymers of 1-vinyl-2-pyrrolidonedivinylbenzene. *J. Therm. Anal. Calorim.* **2013**, *114*, 749–755. [[CrossRef](#)]
57. Maciejewska, M.; Szajnecki, Ł.; Gawdzik, B. Investigation of the surface area and polarity of porous copolymers of maleic anhydride and divinylbenzene. *Appl. Polym. Sci.* **2012**, *125*, 300–307. [[CrossRef](#)]
58. Gawdzik, B. Studies on the selectivity of porous polymers based on polyaromatic esters. *J. Chromatogr. A* **1990**, *503*, 41–49. [[CrossRef](#)]
59. Tuncel, A.; Piskin, E. Nonswellable and Swellable Poly (EGDMA) microspheres. *J. Appl. Polym. Sci.* **1996**, *62*, 789–798. [[CrossRef](#)]
60. Barrett, E.P.; Joyner, L.G.; Halenda, P.H. The Determination of Pore Volume and Area Distributions in Porous Substances. I. Computations from Nitrogen Isotherms. *J. Am. Chem. Soc.* **1951**, *73*, 373–380. [[CrossRef](#)]
61. Arshady, R. In the Name of Particle Formation. *Colloids Surf. A Physicochem. Eng. Asp.* **1999**, *153*, 325–333. [[CrossRef](#)]

**Disclaimer/Publisher's Note:** The statements, opinions and data contained in all publications are solely those of the individual author(s) and contributor(s) and not of MDPI and/or the editor(s). MDPI and/or the editor(s) disclaim responsibility for any injury to people or property resulting from any ideas, methods, instructions or products referred to in the content.